Fore-arc basalts and subduction initiation in the Izu-Bonin-Mariana system

Mark K. Regan, Osamu Ishizuka, Robert J. Stern, Katherine A. Kelley, Yasuhiko Ohara, Janne Blichert-Toft, Sherman H. Bloomer, Jennifer Cash, Patricia Fryer, Barry Hanan, et al.

Geochemistry Geophysics Geosystems G3
AN ELECTRONIC JOURNAL OF THE EARTH SCIENCES
Published by AGU and the Geochemical Society

Article
Volume 11, Number 3
6 March 2010
Q03X12, doi:10.1029/2009GC002871
ISSN: 1525-2027

Fore-arc basalts and subduction initiation in the Izu-Bonin-Mariana system

Mark K. Reagan
Department of Geoscience, University of Iowa, Iowa City, Iowa 52242, USA (mark-reagan@uiowa.edu)

Osamu Ishizuka
Institute of Geoscience and Geoinformation, Geological Survey of Japan, AIST, Central 7, 1-1-1, Higashi, Tsukuba, Ibaraki 305-8567, Japan

Robert J. Stern
Geoscience Department, University of Texas at Dallas, Box 830688, Richardson, Texas 75083-0688, USA

Katherine A. Kelley
Graduate School of Oceanography, University of Rhode Island, Narragansett, Rhode Island 02882, USA

Yasuhiko Ohara
Hydrographic and Oceanographic Department of Japan, 5-3-1 Tsukiji, Chuo-ku, Tokyo 104-0045, Japan

Janne Blichert-Toft
Laboratoire de Sciences de la Terre, UMR 5570, Ecole Normale Supérieure de Lyon, Université Claude Bernard Lyon 1, CNRS, 46 Allée d'Italie, F-69364 Lyon CEDEX 07, France

Sherman H. Bloomer
Department of Geoscience, Oregon State University, Corvallis, Oregon 97331, USA

Jennifer Cash
Department of Geoscience, University of Iowa, Iowa City, Iowa 52242, USA

Patricia Fryer
Hawaii Institute of Geophysics and Planetology, SOEST, University of Hawai'i at Mānoa, 1680 East-West Road, POST 602, Honolulu, Hawaii 96822, USA

Barry B. Hanan
Department of Geological Sciences, San Diego State University, San Diego, California 92182, USA

Rosemary Hickey-Vargas
Department of Earth Sciences, Florida International University, University Park Campus, Miami, Florida 33199, USA

Teruaki Ishii and Jun-Ichi Kimura
Institute for Research on Earth Evolution, Japan Agency for Marine-Earth Science and Technology, Kanagawa 236-0016, Japan

David W. Peate, Michael C. Rowe, and Melinda Woods
Department of Geoscience, University of Iowa, Iowa City, Iowa 52242, USA

[1] Recent diving with the JAMSTEC *Shinkai 6500* manned submersible in the Mariana fore arc southeast of Guam has discovered that MORB-like tholeiitic basalts crop out over large areas. These "fore-arc basalts" (FAB) underlie boninites and overlie diabasic and gabbroic rocks. Potential origins include eruption at a spreading center before subduction began or eruption during near-trench spreading after subduction began. FAB trace element patterns are similar to those of MORB and most Izu-Bonin-Mariana (IBM) back-arc lavas. However, Ti/V and Yb/V ratios are lower in FAB reflecting a stronger prior depletion of their mantle source compared to the source of basalts from mid-ocean ridges and back-arc basins. Some FAB also have higher concentrations of fluid-soluble elements than do spreading center lavas. Thus, the most likely origin of FAB is that they were the first lavas to erupt when the Pacific Plate began sinking beneath the Philippine Plate at about 51 Ma. The magmas were generated by mantle decompression during near-trench spreading with little or no mass transfer from the subducting plate. Boninites were generated later when the residual, highly depleted mantle melted at shallow levels after fluxing by a water-rich fluid derived from the sinking Pacific Plate. This magmatic stratigraphy of FAB overlain by transitional lavas and boninites is similar to that found in many ophiolites, suggesting that ophiolitic assemblages might commonly originate from near-trench volcanism caused by subduction initiation. Indeed, the widely dispersed Jurassic and Cretaceous Tethyan ophiolites could represent two such significant subduction initiation events.

Components: 11,923 words, 8 figures, 2 tables.

Keywords: Mariana; fore arc; basalt; geochemistry; ophiolite.

Index Terms: 1031 Geochemistry: Subduction zone processes (3060); 1065 Geochemistry: Major and trace element geochemistry; 1040 Geochemistry: Radiogenic isotope geochemistry.

Received 22 September 2009; **Revised** 10 December 2009; **Accepted** 30 December 2009; **Published** 6 March 2010.

Reagan, M. K., et al. (2010), Fore-arc basalts and subduction initiation in the Izu-Bonin-Mariana system, *Geochem. Geophys. Geosyst.*, *11*, Q03X12, doi:10.1029/2009GC002871.

Theme: Izu-Bonin-Mariana Subduction System: A Comprehensive Overview
Guest Editors: S. Kodaira, S. Pozgay, and J. Ryan

1. Introduction

[2] On-land studies of the Bonin and Mariana fore-arc islands, as well as drilling, diving, and dredging along submarine portions of the Izu-Bonin-Mariana (IBM) fore arc has recovered suites of subduction-related volcanic rocks with ages of 49–43 Ma and compositions that are distinct from those of the modern volcanic arc [*Bloomer*, 1983; *Bloomer and Hawkins*, 1987; *Hickey-Vargas*, 1989; *Ishizuka et al.*, 2006; *Komatsu*, 1980; *Kuroda and Shiraki*, 1975; *Meijer*, 1980; *Pearce et al.*, 1992; *Reagan and Meijer*, 1984; *Taylor et al.*, 1994; *Umino*, 1985]. These lavas are widely accepted to have formed in extensional environments shortly after IBM subduction began. Heretofore, the most abundant of these fore-arc volcanics have been thought to be boninites and high-Mg andesites. This supposition is based on the coincidence of the oldest of these ages with the estimated timing of a major change in motion of the Pacific Plate [*Cosca et al.*, 1998; *Ishizuka et al.*, 2006; *Meijer et al.*, 1983], the unusual compositions of these lavas [*Falloon and Danyushevsky*, 2000; *Meijer*, 1980; *Stern and Bloomer*, 1992], and their widespread outcroppings on fore-arc islands [*Reagan and Meijer*, 1984; *Umino*, 1985].

[3] Tholeiitic basalts also have been found in the IBM fore arc. Some of these basalts are interbedded with or overlie boninites [*Reagan and Meijer*, 1984; *Taylor and Nesbitt*, 1994], and have trace element and isotopic characteristics similar to low-K arc tholeiitic basalts from many volcanic arcs [see *Gill*, 1981]. However, recent diving with the *Shinkai 6500* manned submersible in the Mariana fore arc southeast of Guam has discovered that vast areas of the deep fore arc are floored by tholeiitic basalts with geochemical attributes more akin to mid-ocean ridge basalts (MORB) than to arc tholeiites. Indeed, the most abundant rock type between 6500 and

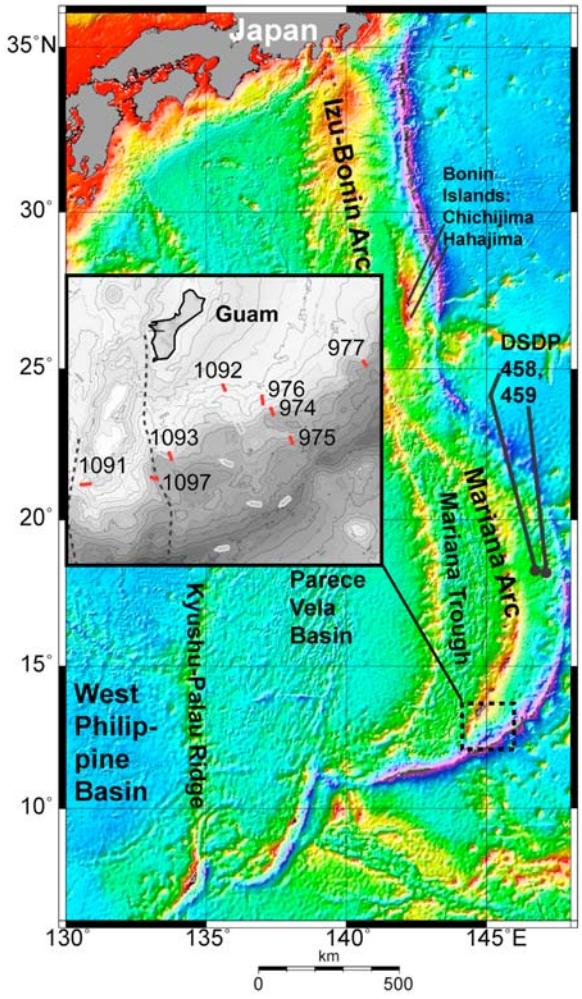

Figure 1. Location map for the IBM arc province. Inset is a bathymetric map of the Mariana fore arc southeast of Guam where *Shinkai 6500* diving was conducted. Dive sites are shown with red lines and labeled with their number. The official numbers for dives 974–977 have a "YK06-12-" prefix, and those for dives 1091–1097 have a "YK08-08-" prefix. The dashed line running between the escarpment immediately west of Guam and the trench is the East Santa Rosa Banks Fault [*Fryer et al.*, 2003].

2000 m depth in this area appears to be basaltic pillow lavas and associated shallow intrusives [*Ohara et al.*, 2008]. Because these lavas have geochemical affinities with lavas erupted at spreading centers and they are found in the present-day fore arc, we hereafter term these lavas "fore-arc basalts" (FAB). Similar basalts, which we reinterpret here as FAB, were encountered beneath boninitic lavas at DSDP drill site 458 [*Meijer*, 1980; *Meijer et al.*, 1982], during *Shinkai 6500* diving in the Bonin fore arc [*DeBari et al.*, 1999], and near Hahajima Seamount [*Ishiwatari et al.*, 2006]. In all of these locations, FAB underlie and/or are trenchward of boninites and younger arc lavas. The wide distribution of these basalts suggests that they are significantly more voluminous than has previously been recognized, and indeed, these basalts might be the most abundant volcanic rocks in the IBM fore arc. We show below that these rocks have compositional differences with arc tholeiites as well as back-arc basalts from the Philippine Plate and mid-ocean ridge basalts, and we postulate that these lavas are the first lavas to erupt after subduction begins.

2. Mariana Fore-Arc Geology

[4] During the summers of 2006 and 2008, 12 dives of the JAMSTEC manned submersible *Shinkai 6500* were undertaken along the southern Mariana fore arc, eight of which explored fore-arc lithologies east of the westernmost N–S fault bounding the Mariana Trough near 144°10′E (the East Santa Rosa Banks Fault (Figure 1 and Table 1)). This fault is thought to approximate the position of a tear in the subducted slab [*Fryer et al.*, 2003; *Gvirtzman and Stern*, 2004]. The region to the west is dominated by back-arc basin extension, active magmatism, and rapid deformation [*Martinez et al.*, 2000] in contrast to the stable fore arc to the east, which is the location of this study and is herein termed the SE Mariana fore arc.

[5] From east to west and bottom to top, the sequence of lithologies we have observed or compiled from the SE Mariana fore arc appears to be peridotite, gabbro, and related intrusive rocks, FAB and associated diabase, boninite, and younger subduction-related lavas [*Ohara et al.*, 2008]. The position of FAB beneath boninite is confirmed by the stratigraphy encountered at DSDP drill site 458 in the Mariana fore arc near 18°N (Figure 1), where the lowermost 50 m of drill core are pillow lavas with incompatible trace element abundances similar to those of FAB from the dive sites [*Hussong et al.*, 1982]. The overlying 50 m of core consists of FAB pillow lavas interbedded with pillow lavas that are transitional between FAB and boninite. The remaining igneous section of the site 458 drill core consists entirely of transitional lavas.

3. Petrography

[6] The FAB samples collected from the 2006 and 2008 dive sites in the SE Mariana fore arc are fragments of pillow lavas and shallow diabasic intrusions. True phenocrysts or large crystals are rare, and when present, typically are euhedral to

Table 1. Dive Sites and Recovered Lithologies

Dive	Latitude	Longitude	Depths	Igneous Lithologies
YK06-12, 974	12°55.2345′–12°55.9862′	145°18.9270′–145°18.7998′	6270–5757	FAB, Diabase, Boninite, Arc lavas
YK06-12, 975	12°47.1764′–12°48.1224′	145°28.9198′–145°28.7107′	6489–5892	FAB, Diabase, Gabbro
YK06-12, 976	13°2.0952′–13°3.7499′	145°20.5585′–145°19.4416′	3802–3079	FAB, Diabase, Arc lavas
YK06-12, 977	13°16.4609′–13°17.2571′	145°56.7032′–145°56.0253′	6363–5483	FAB, Diabase
YK08-08, 1091	12°35.4239′–12°35.4466′	144°14.6270′–144°16.0581′	2696–1958	FAB, Diabase, Arc lavas
YK08-08, 1092	12°6.1786′–12°6.9853′	145°9.1768′–145°9.1679′	3000–2600	FAB, Diabase, Arc lavas
YK08-08, 1093	12°40.1963′–12°40.8024′	144°43.7479′–144°43.9026′	6441–5798	FAB, Diabase
YK08-08, 1097	12°34.7322′–12°34.7955′	144°39.8224′–144°39.1740′	6494–5978	FAB, Diabase, Boninite

skeletal olivine pseudomorphed by iddingsite. Glassy pillow rinds have less than one to several percent acicular and skeletal plagioclase crystals, sometimes in crystal clots with acicular augite. Interiors of pillow lavas consist of quench-textured intergrowths of acicular to skeletal plagioclase that are less than a few tenths of a millimeter long, smaller granular to acicular augite, and granular magnetite (Figure 2). The acicular plagioclase and augite intergrowths often form patchy radiating or sheaf-like crystal clots in the pillow rinds. The quenched texture of FAB plagioclase and augite is reminiscent of the spinifex texture seen in komatiites, but plagioclase is the dominant mineral instead of olivine and the scale is microscopic. A saponite clay groundmass after glass makes up a few to tens of percent of the pillow interiors. The pillow lavas have 0–10% vesicles. Some of the spinifex-like samples are dictytaxitic.

[7] FAB encountered in the lower cores at DSDP sites 458 and 459 have similar textures to FAB from the dive sites, although the pillow rinds are more crystalline. The uppermost cores consist of pillow lavas with abundant microphenocrysts of augite set in a glassy to fine grained matrix. These lavas previously have been categorized as boninites

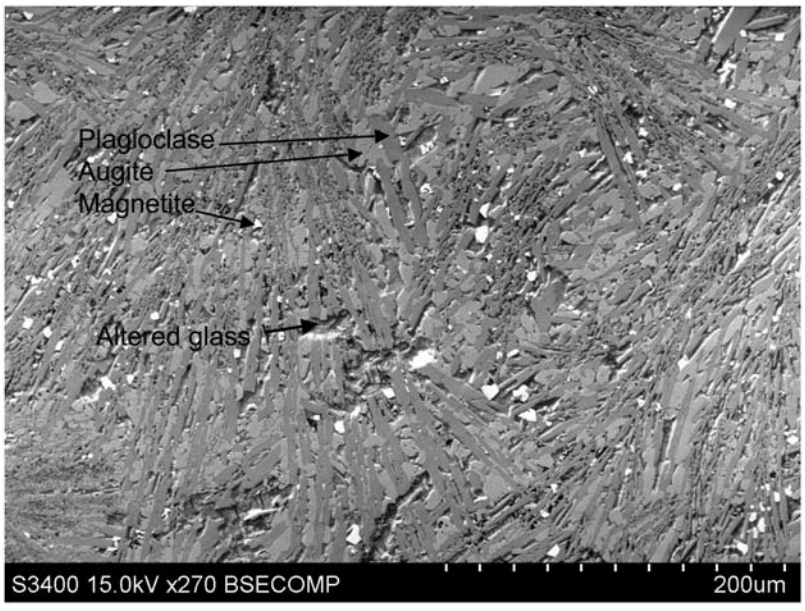

Figure 2. Backscatter image of a polished thin section from FAB sample YK06-12-975-R27. Scale is at the bottom right. The brightest grains are magnetite, followed by clinopyroxene and plagioclase. Interstices between grains are largely filled by clays after original volcanic glass.

[e.g., *Meijer*, 1980; *Hickey and Frey*, 1982], but, as will be shown below, they are probably transitional between FAB and true boninite.

[8] The FAB diabase samples have subophitic textures consisting of intergrown acicular to lath-shaped plagioclase, anhedral to subhedral augite, and skeletal to granular magnetite. Vesicles are absent in some samples but can make up several % of some diabase samples.

4. Analytical Methods

[9] Several laboratories were involved in generating the data in Table 2. Glassy pillow rind fragments were analyzed for major elements by a Cameca SX100 electron microprobe at Oregon State University using a 5 micron spot size, a 30 nA beam current and a 15 keV accelerating voltage [*Rowe et al.*, 2007]. Each reported analysis is an average of 10 spot analyses. Na, Si, and K time = 0 intercept corrections were used for each spot analysis.

[10] Trace element concentrations for these pillow rind fragments were obtained by laser ablation ICPMS, using either the Merchantek/VG MicroProbeII LUV 213 nm Nd-YAG laser and VG PQ ExCell quadrupole ICP-MS at Boston University or the New Wave UP 213 nm Nd-YAG laser and Thermo X-Series II quadrupole ICP-MS at the Graduate School of Oceanography, University of Rhode Island following techniques outlined by and adapted from [*Kelley et al.*, 2003]. Analysis spots were chosen to avoid visible crystals in the glass, but microphenocryst abundances in some of the DSDP samples were high enough that crystals were incorporated during ablation; in most cases these were readily identified as spikes in the laser data and removed from the data. Laser spot sizes were 80–120 μm diameter, and 8–12 separate spots were analyzed per glass sample. Raw time-resolved laser data were background subtracted, normalized to ^{47}Ti as an internal standard, and calibrated ($R^2 > 0.99$) against USGS basaltic glass standards BIR-1G, BHVO-2G, and BCR-2G ± MPI-DING glass standards KL2-G, ML3B-G, StHls-G, GOR128-G, and T1-G.

[11] Major and trace element data for whole rocks from the 2008 dive sites (dive numbers: 1091–1097) were obtained at the Geological Survey of Japan using techniques described by *Ishizuka et al.* [2006]. Similar data for DSDP sites 458 and 459 were collected at the University of Kansas [*Elliott et al.*, 1997; *Plank and Ludden*, 1992]. Whole rocks from 2006 dive sites (974–977) were analyzed for major and trace elements at Washington State University using XRF [*Johnson et al.*, 1999] and ICP-MS (http://www.sees.wsu.edu/Geolab/note/icpms.html) techniques, respectively.

[12] Sr, Nd, Pb and Hf isotopes for the DSDP whole rock and glass samples were obtained at San Diego State University and Ecole Normale Superieure in Lyon using techniques described by *Blichert-Toft et al.* [1997], *Hanan and Schilling* [1989], *Reagan et al.* [2008], and *White et al.* [2000]. Hf and Pb isotopic compositions were measured in Lyon using a VG Plasma 54 MC-ICP-MS, whereas Sr and Nd isotopes were analyzed at San Diego State University using a VG Sector 54 Thermal Ionization Mass Spectrometer (TIMS) and a Nu Plasma HR MC-ICP-MS, respectively. The Pb isotope ratios for these samples were corrected for instrumental mass fractionation and machine bias by applying a discrimination factor determined by bracketing sample analyses with analyses of the NIST standard SRM 981. NIST SRM 997 Tl was used to monitor mass fractionation.

[13] Sr, Nd and Pb isotope data for the dive samples were acquired utilizing a 9 collector VG Sector 54 mass spectrometer at the Geological Survey of Japan and techniques described by *Ishizuka et al.* [2009]. Mass fractionation during the Pb isotopic analyses was monitored using a double spike (Southampton-Brest Lead 207–204 spike (SBL74)).

[14] The procedures and data handling for the Hf isotope analyses for the dive rocks are described in additional detail here, as they are the first results reported from the University of Iowa group. The chemical procedures to extract and purify Hf for whole rocks from the dive sites were based on those published online by the Geosciences Department at Boise State University (http://earth.boisestate.edu/isotope/labshare.html). Sample powders (100–300 mg) were digested in a mixture of concentrated HNO_3 and HF. After evaporation and two dissolutions in HNO_3 and evaporations, the sample residues were converted to a chloride form by adding a few milliliters of 6N HCl and evaporation. The samples were then dissolved in 5 ml of 0.1 M HF-1.0 M HCl. The column chemistry procedure is based on the procedures published by *Münker et al.* [2001]. Each sample was dissolved in a 2% nitric acid solution for analysis.

[15] The mass spectrometry for Hf was done at the University of Illinois using MC-ICP-MS techniques patterned after *Lu et al.* [2007]. Normalization was to a ^{179}Hf/^{177}Hf ratio of 0.7325. The DLC Hf standard was analyzed every two to four samples. All analyses were corrected for drift to a

Table 2 (Sample). Major Element, Trace Element, and Isotopic Data for Samples From *Shinkai 6500* Dive Sites and DSDP Sites 447, 458, and 459[a] [The full Table 2 is available in the HTML version of this article]

	Sample[b]									
	974-R9g	974-R10g	974-R10	975-R22	975-R26	975-R27	977-R19	1091-18	1092-1	1092-9
Rock type[c]	FAB	FAB	FAB	FAB	FAB	FAB	FAB	FAB	FAB	FAB-D
SiO_2	51.19	51.13	50.91	51.92	50.17	50.26	49.12	49.99	50.03	50.81
TiO_2	1.02	1.02	0.96	1.64	0.98	1.02	1.01	0.67	1.11	1.08
Al_2O_3	14.18	14.13	14.45	14.61	15.82	16.37	15.73	15.33	14.92	14.58
FeO[d]	12.26	12.44	11.90	14.16	10.48	9.89	12.01	8.88	11.73	11.64
MnO	0.23	0.20	0.21	0.18	0.15	0.15	0.17	0.14	0.14	0.15
MgO	7.56	7.47	7.33	4.62	7.21	6.55	7.15	9.76	7.33	8.30
CaO	11.45	11.54	11.87	9.19	12.39	13.00	12.02	12.93	11.98	11.03
Na_2O	1.95	1.92	2.14	3.14	2.43	2.46	2.53	2.17	2.42	2.23
K_2O	0.074	0.070	0.14	0.40	0.29	0.22	0.15	0.07	0.24	0.08
P_2O_5	0.08	0.08	0.09	0.14	0.08	0.08	0.09	0.05	0.10	0.09
Total[e]	100.28	100.31	97.54	95.33	95.93	95.25	95.57	96.33	97.64	97.41
Li	6.32	5.64	–	–	–	–	–	–	–	–
Cs	0.02	0.02	0.04	4.21	0.33	0.11	0.08	0.09	0.42	0.00
Rb	1.45	1.39	1.68	30.22	4.43	2.13	1.51	0.901	5.18	0.40
Ba	19.6	19.3	23.5	18.9	6.3	5.4	4.6	2.0	10.0	5.2
Sr	63.9	62.9	61.5	95.4	69.5	71.0	72.0	67.5	75.7	70.3
Pb	0.28	0.25	0.63	0.13	0.25	0.24	0.23	0.11	0.21	0.13
Th	0.18	0.18	0.19	0.32	0.14	0.14	0.14	0.05	0.14	0.12
U	0.05	0.05	0.05	0.17	0.13	0.08	0.06	0.05	0.25	0.06
Nb	2.22	2.22	1.84	4.29	1.45	1.52	1.46	0.62	1.88	1.61
Ta	0.14	0.14	0.12	0.29	0.10	0.10	0.10	0.04	0.12	0.10
La	2.10	2.15	1.92	4.10	1.62	1.70	2.04	0.94	2.06	1.73
Ce	6.08	5.97	5.32	10.52	4.87	5.16	5.20	3.19	6.38	5.35
Pr	1.03	1.03	0.91	1.65	0.88	0.93	0.98	0.52	1.02	0.88
Nd	5.67	5.84	5.12	8.73	5.06	5.40	5.59	3.16	5.76	5.37
Zr	48.9	51.7	44.3	77.3	48.9	50.9	47.1	30.0	60.0	56.6
Hf	1.54	1.63	1.40	2.32	1.51	1.61	1.53	0.84	1.72	1.57
Sm	2.25	2.31	2.07	3.07	2.12	2.30	2.25	1.28	2.27	2.20
Eu	0.86	0.88	0.85	1.24	0.87	0.90	0.89	0.52	0.83	0.80
Gd	3.64	3.78	3.27	4.28	3.29	3.49	3.51	1.81	3.40	3.22
Tb	0.68	0.71	0.66	0.81	0.66	0.71	0.70	0.36	0.69	0.63
Dy	4.55	4.80	4.66	5.65	4.67	4.97	5.00	2.42	4.64	4.39
Ho	1.03	1.08	1.03	1.25	1.02	1.12	1.11	0.58	1.06	1.03
Er	3.07	3.22	3.01	3.54	2.93	3.20	3.11	1.70	3.27	3.05
Tm	0.49	0.51	0.45	0.54	0.43	0.48	0.47	0.27	0.50	0.49
Yb	3.17	3.30	2.87	3.43	2.75	3.05	2.91	1.73	3.31	3.20
Lu	0.50	0.52	0.46	0.56	0.42	0.49	0.46	0.26	0.51	0.48
Y	26.0	27.7	26.1	31.6	24.8	28.4	27.9	16.6	31.0	29.6
V	401	383	369	451	364	377	369	252	418	428
Sc	–	–	50.3	31.6	56.4	56.9	47.7	–	–	–
Ni	93	83	83	27	93	82	56	246	72	123
Cr	255	241	246	16	322	312	100	682	285	269
Co	55	51	–	–	–	–	–	–	–	–
Cu	208	194	161	23	178	200	181	–	–	–
$^{87}Sr/^{86}Sr$	–	–	0.703114	0.702820	0.702817	0.702824	0.702888	0.703476	0.702888	0.703217
$^{143}Nd/^{144}Nd$	–	–	0.513125	0.513177	0.513218	0.513198	0.513193	0.513112	–	0.513172
$^{176}Hf/^{177}Hf$	–	–	0.283309	–	0.283311	0.283311	0.283270	0.283259	–	0.283272
$^{206}Pb/^{204}Pb$	–	–	18.0570	18.0178	18.3102	18.3935	18.1160	18.4516	18.3063	18.1381
$^{207}Pb/^{204}Pb$	–	–	15.4429	15.4262	15.4248	15.4531	15.4437	15.5202	15.4407	15.4356
$^{208}Pb/^{204}Pb$	–	–	37.6050	37.7933	37.9544	38.0012	37.9425	38.3162	37.9078	37.8179

[a]Element data are in wt %, and trace element data are in ppm.
[b]Sample numbers ending in "g" are hand-picked glasses.
[c]FAB, fore-arc basalt; D, diabase; Bon, boninite; Trans, transitional lava between Bon and FAB; WPB, West Philippine Basin basalt.
[d]Total Fe as FeO.
[e]Total before normalization.

$^{176}Hf/^{177}Hf$ value of 0.281878 for the DLC standard, which is the published value for this standard relative to a value of 0.282160 for JMC-475 [see *Ulfbeck et al.*, 2003]. The average counting statistical error on the sample values was 0.000004. Blanks were approximately 10 pg, and no correction was made for the blank. BHVO-1 was analyzed 5 times along with the samples, yielding an average $^{176}Hf/^{177}Hf$ value and standard deviation of 0.283094 ± 0.000003. A measurement of $^{176}Hf/^{177}Hf$ for BHVO-1 from Lyon yielded 0.283109 ± 0.000004 [*Blichert-Toft et al.*, 1999], suggesting that the Iowa-Illinois data are systematically lower than the Lyon data by 1/2 epsilon unit.

5. Geochemistry

[16] The major element compositions of FAB whole rocks and glasses from the dive sites span a relatively narrow range, with SiO_2 = 49–51 wt %, Al_2O_3 = 14–17 wt %, CaO = 10–13 wt %, and MgO = 4–8 wt % (Table 2). These lavas are tholeiitic with FeO*/MgO = 0.9–3.0. Na_2O concentrations in whole rocks are somewhat variable, reflecting seafloor alteration. Ni and Cr concentrations range from 27 to 246 and 16 to 682 ppm, respectively (Table 2). Rare earth element (REE) patterns (Figure 3) are like those of mid-ocean ridge basalts (MORB), with most La/Yb ratios varying between 0.5 and 0.9. Ratios between high field strength elements (HFSE; i.e., Zr, Hf, Nb, Ta, Ti) and REE also are similar to those of MORB. However, ratios between REE or HFSE and V (e.g., Ti/V and Yb/V (Figure 4)) are lower in FAB than in MORB and most back-arc basin lavas but are similar to those measured in subduction related basalts. Concentrations of K, Rb, U and other "fluid soluble" elements are highly variable in FAB, such that ratios of these elements to light REE (e.g., Rb/La, U/La) range from MORB-like to arc-like (Table 2). The two analyses of pure FAB glasses are the most MORB-like, suggesting that the fluid-soluble element enrichment in some dive site whole rock samples resulted from seafloor alteration [cf. *Kelley et al.*, 2003].

[17] Dive site boninites are similar in composition to those reported from the type location of boninites at Chichijima [*Pearce et al.*, 1999; *Taylor et al.*, 1994; *Umino*, 1985]. They are magnesian (MgO = 10.6–15.5 (Table 2)) andesites (SiO_2 = 54.7–57.1 wt %) with exceedingly low concentrations of TiO_2 (0.15–0.38 wt %) and REE (Figure 3). CaO (5.1–9.4 wt %) and Al_2O_3 (10.7–13.2 wt %) concentrations are significantly lower than those of the FAB. Concentrations of many fluid soluble elements as well as Zr and Hf are enriched over the REE in these boninites (Figure 4).

[18] DSDP site 458 and 459 lavas have compositions that are transitional between those of FAB and true boninites. The lowermost site 458 lavas and all site 459 lavas have whole-rock compositions that are FAB-like, but are more silicic (SiO_2 = 52–54 wt %). Pillow rind glass compositions for these lavas are andesitic reflecting the presence of plagioclase and clinopyroxene crystals. The REE and HFS element concentrations of the DSDP samples are nearly identical to those of the FAB (Figure 3), as are Ti/V and Yb/V ratios (Figure 4). However, The fluid soluble elements Cs, K, Rb, Ba, Sr, Pb, and U are clearly enriched in these isotropic FAB glasses (Figure 3 and Table 2). Up-section at site 458, the FAB become interbedded with lavas that have lower REE concentrations and flatter REE patterns, eventually transitioning to lavas with REE and HFS concentrations that are about as depleted as those of boninities from IBM locations, except that they remain depleted in light versus heavy REE, whereas nearly all IBM boninites are LREE enriched, including those encountered in the diving (Figure 3) [*Hickey-Vargas and Reagan*, 1987; *Ishizuka et al.*, 2006; *Pearce et al.*, 1999; *Taylor et al.*, 1994]. The major element concentrations of these lavas also are not entirely boninitic, as they are neither particularly magnesian nor silicic, and they have higher CaO and Al_2O_3 concentrations than the dive site boninites. We therefore interpret these lavas to be transitional between true boninites and FAB. All of the glasses from the transitional lavas have concentrations of the fluid-soluble elements that are similar to those of the FAB glasses (see Figure 3b) suggesting that all of the enrichments in these elements in these glasses resulted from fluid fluxing from the subducting slab.

[19] High-Ca boninites and other high-Mg andesites found atop low Ca boninites on Chichijima [*Ishizuka et al.*, 2006; *Taylor et al.*, 1994; *Umino*, 1985] and upslope from the dive sites on Guam [*Reagan and Meijer*, 1984] have a separate origin from the transitional lavas at DSDP site 458. These younger lavas have light REE enriched patterns, and have incompatible trace element ratios (e.g., Ba/La, La/Nb) that are more akin to arc lavas than to FAB. Their genesis reflects a transition from the processes and sources that generated boninites (i.e., highly depleted mantle source, high degrees of fluxed melting at shallow levels) toward those responsible for normal arc volcanism [*Ishizuka et al.*, 2006; *Reagan et al.*, 2008].

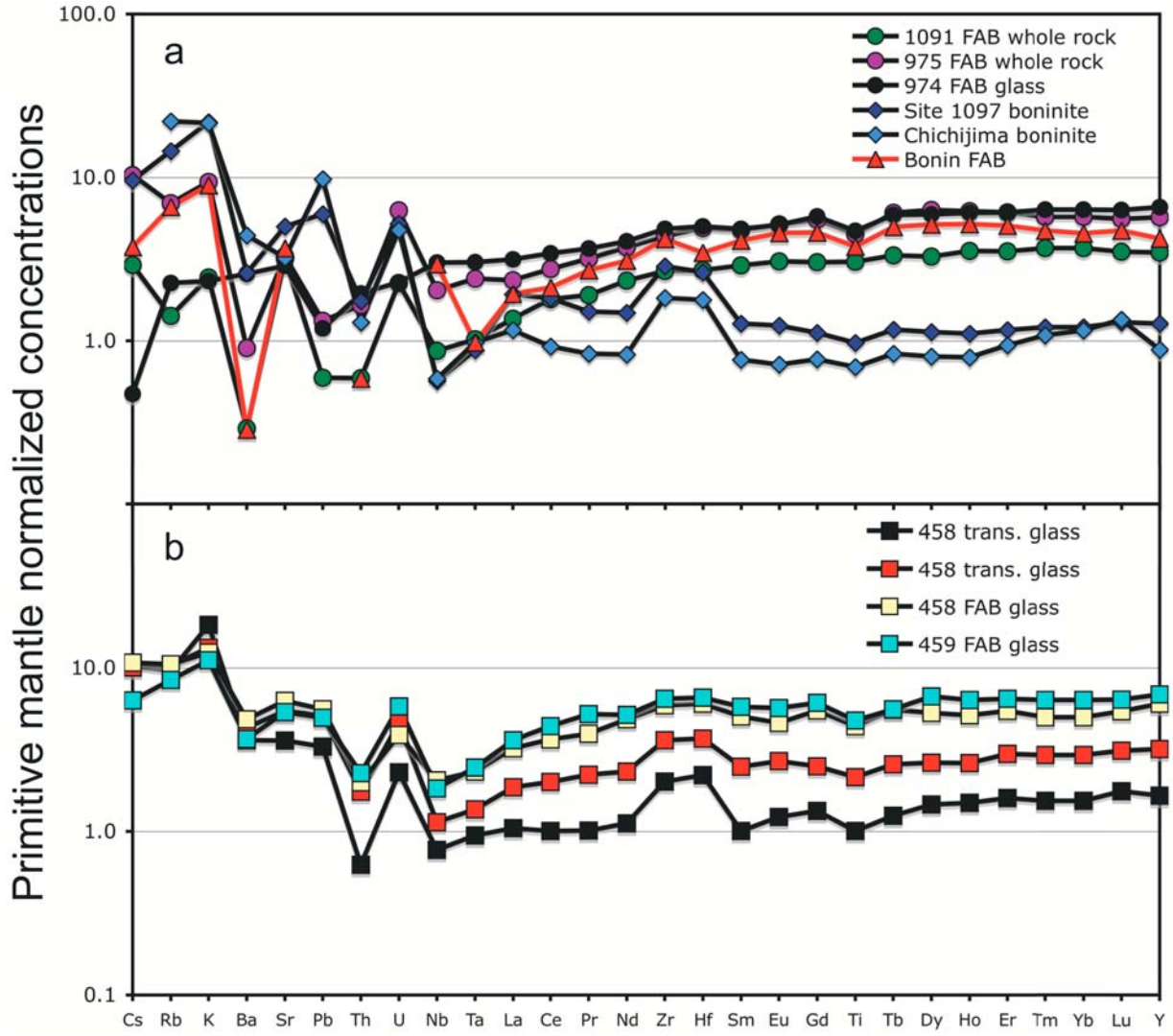

Figure 3. Primitive mantle [*Sun and McDonough*, 1989] normalized concentrations of incompatible trace elements for whole rocks and glasses from (a) *Shinkai 6500* dive sites (b) and DSDP sites 458 and 459. Data are from Table 2. Also included in Figure 3a are a boninite from Chichijima [*Pearce et al.*, 1999] and a representative basalt from the Bonin trench slope [*DeBari et al.*, 1999]. The elements are arranged such that those commonly thought to be transferred abundantly from the subducting slab to the mantle sources of arc lavas are to the left and less abundantly transferred REE and HFS elements are to the right.

[20] Nd isotope ratios for FAB from the dive sites are bimodal and vary according to the locations of the dives. Samples from the more northeasterly dives 974–977 and 1092 have higher $^{143}Nd/^{144}Nd$ (0.513170–0.513218), whereas samples from the more southwesterly dives 1091, 1093, and 1097 have lower $^{143}Nd/^{144}Nd$ (0.513096–0.513112). The Nd isotope values for the northeasterly dives are more radiogenic than all Philippine Plate back-arc lavas, whereas the southwesterly dives have values that overlap with the back-arc lavas. On a plot of Nd versus Sr isotopic compositions (Figure 5), the southwesterly dive samples plot along a linear trend between the northeasterly samples and the FAB to transitional samples from DSDP sites discussed below. This trend is offset to higher Sr isotope values than most Philippine Plate back-arc basin basalts and other oceanic lavas, although the Sr and Nd isotopic compositions of some West Philippine Basin lavas plot within the field defined by the SE Mariana fore-arc FAB.

[21] The Nd isotope values for the dive site boninites lack the bimodal distribution observed for the

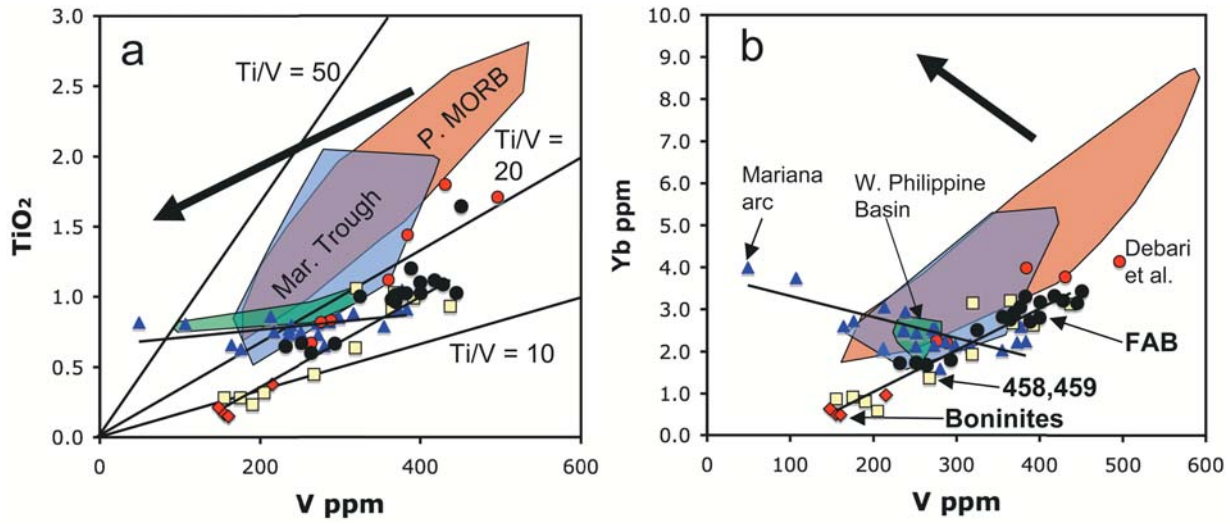

Figure 4. Plot of (a) wt % TiO_2 and (b) Yb ppm against V ppm for Mariana fore-arc and arc lavas. FAB from the dive sites are shown with black circles. Lavas from DSDP sites 458 and 459 are shown with yellow squares. Lavas from the Bonin fore arc [*DeBari et al.*, 1999] are shown with red circles. Dive site boninites are shown with red diamonds. These data are from Table 2. Active arc lavas [*Elliott et al.*, 1997; *Woodhead et al.*, 2001] are shown with dark blue triangles. Basalts from the East Pacific Rise and from the Mariana Trough are illustrated in the brown and blue fields, respectively. Data and references for these sample suites are from the PetDB database (http://www.petdb.org/). The field for the WPB [*Pearce et al.*, 1999; *Savov et al.*, 2006] also is shown in green. This field includes sample 447A 14-1 from Table 2. Blue lines in Figure 4a show Ti/V ratios. Fine black lines are linear regressions through the data for the lavas from DSDP sites 458 and 459 and from the active arc. Thick black arrows illustrate the differentiation trends when magnetite is part of the crystallizing assemblage.

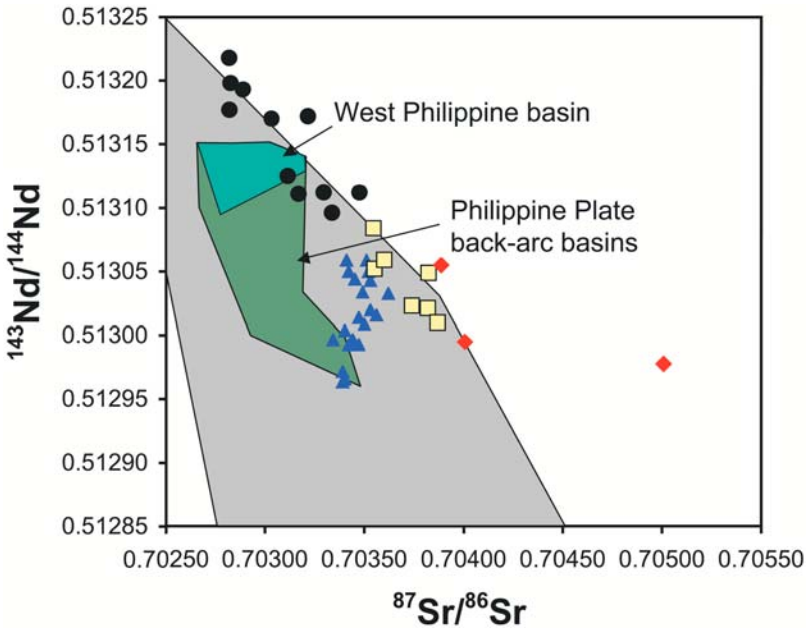

Figure 5. Plot of Sr and Nd isotopic compositions for Mariana fore-arc and arc lavas. Data for the WPB and other Philippine Plate are from *Volpe et al.* [1990], *Hickey-Vargas* [1991], and *Savov et al.* [2006]. The field for modern MORB and ocean island basalts from the Pacific and Indian Ocean regions is illustrated as a pale gray field. Other data sources and symbols are the same as in Figure 4.

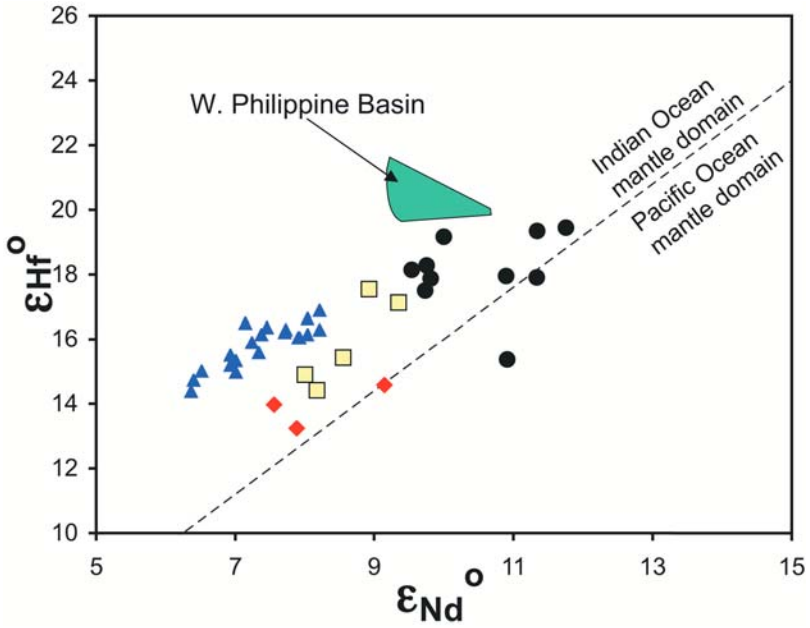

Figure 6. Plot of initial ε_{Hf} against ε_{Nd} for Mariana fore-arc lavas. The isotope values were corrected for 50 million years of radiogenic ingrowth. Values of ε_{Hf} and ε_{Nd} were calculated by normalizing to 50 Ma CHUR values of $^{176}Hf/^{177}Hf = 0.282737$ and $^{143}Nd/^{144}Nd = 0.512574$, respectively. The ε_{Hf} values for the dive site samples were calculated from the values listed in Table 2 and then adjusted upward 0.5 units to account for the offset in BHVO-1 data collected at Lyon and Iowa-Illinois. Symbols and data sources are the same as in Figure 5.

FAB despite their sampling locations in the northeast and southwest dive sites. These values overlap with those of the DSDP site transitional lavas and extend to less radiogenic values. Sr isotopic compositions of the boninites range from the most radiogenic values found in the transitional lavas from the DSDP sites to significantly more radiogenic values (Table 2 and Figure 5).

[22] Hf isotope compositions of the dive site FAB are somewhat less radiogenic than those of the West Philippine Basin (WPB) and Mariana Trough basalts. On a plot of initial ε_{Nd} and ε_{Hf} (Figure 6), the isotopic compositions for FAB samples from the dives plot in two clusters, consistent with the bimodal Nd isotopic compositions discussed above. The southwestern group of samples have affinities with Indian Ocean MORB (Figure 6) [*Chauvel and Blichert-Toft*, 2001; *Graham et al.*, 2006; *Hanan et al.*, 2004; *Kempton et al.*, 2002] like most other IBM arc, back-arc and fore-arc lavas [*Pearce et al.*, 1999; *Reagan et al.*, 2008]. Most of the northeastern dive site samples plot near the boundary drawn by *Pearce et al.* [1999] between the Indian and Pacific MORB domains, and one falls well within the Pacific domain. FAB samples from DSDP site 458 have initial Nd and Hf isotope values that plot near the southwesterly dive samples. Boninites from all dive sites and the transitional lavas from DSDP site 458 have less radiogenic Nd and Hf isotopic compositions than the FAB, reflecting a source that had lower time-integrated Lu/Hf and Sm/Nd ratios.

[23] Several FAB from the dive sites have Pb isotopic compositions that are similar to those of IBM back-arc lavas [*Hickey-Vargas*, 1998; *Savov et al.*, 2006] and Indian Ocean MORB (Figure 7). Others have more radiogenic Pb isotopic compositions that plot between low $^{206}Pb/^{204}Pb$ IBM back-arc lavas and the more radiogenic Pb isotope values of other early lavas from the IBM fore arc as well as Pacific Ocean floor lavas. This variation is independent of the geographic shift in Nd isotope compositions described above. The FAB from DSDP sites 458 and 459, the transitional lavas, and dive site boninites all have Pb isotopic compositions that plot near the NHRL between typical values for Pacific MORB and those of volcaniclastic sediments from the Pigafeta Basin on the Pacific Plate [see *Meijer*, 1976; *Pearce et al.*, 1999; *Woodhead et al.*, 2001; *Reagan et al.*, 2008].

6. Geochronology

[24] The eruption ages of the FAB must be 49 Ma or older based on the ages of the upper transitional

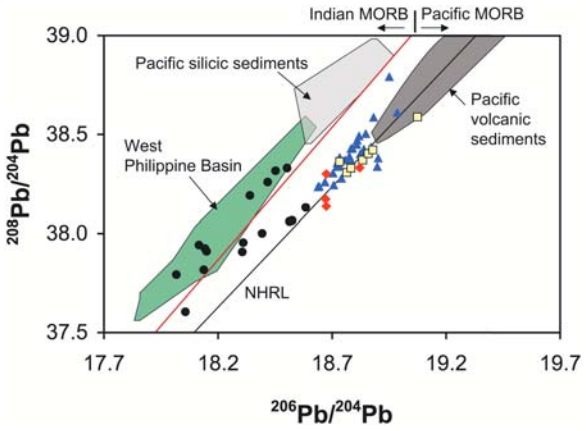

Figure 7. Plot of $^{208}Pb/^{204}Pb$ against $^{206}Pb/^{204}Pb$ for Mariana fore-arc and arc lavas. The medium gray field is for western Pacific Ocean seamounts [*Pearce et al.*, 1999; *Staudigel et al.*, 1991]. The light gray field is for western Pacific silicic sediments [*Ben Othman et al.*, 1989; *Meijer*, 1976; *Pearce et al.*, 1999]. The Northern Hemisphere Regression Line (NHRL) and the dividing line between Indian and Pacific MORB [*Pearce et al.*, 1999] are shown. Other symbols and sources of data are as in Figure 4.

lavas at DSDP site 458 [*Cosca et al.*, 1998], the boninites on Chichijima [*Ishizuka et al.*, 2006], and our geological interpretation placing the FAB beneath boninites along the entire IBM fore arc. Attempts to date the FAB directly in the area southwest of Guam and at DSDP sites 458 and 459 by $^{40}Ar/^{39}Ar$ methods have not been successful, both because of the low K contents of the rocks and because of the alteration of the samples. The Ar age spectra for these samples typically did not yield robust plateaus, intercepts of inverse isochrons typically did not yield atmospheric values, and total gas ages ranged from 19 to 47 Ma (data are available by request from the first author). We infer that the FAB are not much older than the boninites based on the presence of the transitional lavas at DSDP site 458, which indicates that the generation of the FAB and boninites are linked in time and space and by a change in the conditions and sources of melting. There were also no discernible hiatuses encountered between FAB and overlying boninites in the dives or at DSDP site 458 (e.g., unconformities or significant interlayered sedimentary rocks). The most reliable radiometric age for FAB is 51–52 Ma based on one robust $^{40}Ar/^{39}Ar$ plateau age from a pillow lava groundmass, and one U-Pb age on zircon from a FAB-related diabase [*Ishizuka et al.*, 2008]. Both of these samples were collected by *Shinkai 6500* diving in the IBM fore arc east of the Bonin Islands.

7. Discussion

[25] *DeBari et al.* [1999] interpreted MORB-like lavas along the Bonin Trench slope to be part of the WPB crust that were rafted to their present position by back-arc spreading. In this paper we argue that instead, such MORB-like basalts are FAB that were the first lavas to erupt after subduction of the Pacific Plate began. This is based on two lines of reasoning. First, the trace element and isotope compositions of the FAB differ from the compositions of nearly all WPB lavas and other IBM back-arc basin basalts in the system. Second, the petrological link between the FAB and boninites at DSDP site 458 ties both to the time after subduction was initiated.

[26] The aphyric textures of most FAB imply that they were near their liquidus temperatures when they erupted. However, FeO*/MgO values and Ni and Cr concentrations vary significantly, ranging from those expected for near-primary melts of lherzolitic mantle to those that have undergone significant fractionation of olivine and clinopyroxene. The presence of glassy rinds on some fragments indicates that they were erupted subaqueously and their variable vesicularity suggests that many or most FAB were saturated in a vapor phase.

[27] Major and trace element data for FAB demonstrate that they have clear affinities with MORB and BAB lavas. However, their low Ti/V and Yb/V ratios differentiate them from other lavas related to seafloor spreading, and suggest they are more akin to subduction-related lavas such as boninites and arc basalts. The low Ti/V FAB in these subduction-related lavas have been attributed to the oxidized nature of their sources and the resulting high valency and incompatibility of V [*Shervais*, 1982]. However, positive slopes formed by plots of V against TiO_2 for basalts from back arcs and mid-ocean ridges as well as early arc boninites (Figure 4a), suggest that Ti and V are both incompatible in minerals during melting of mantle in subduction and non-subduction-related extensional tectonic settings. This observation is consistent with evidence that V generally has a + 4 valence during melting of the Earth's mantle in most tectonic settings [*Karner et al.*, 2006] and that sources of MORB and relatively primitive arc lavas have similar V/Sc systematics [*Lee et al.*, 2005]. The

similar positive slopes on plots of V against TiO_2 and Yb (Figure 4) demonstrate that all three of these elements can be considered moderately incompatible in basalts from all extensional tectonic environments. Only in significantly differentiated lavas, particularly andesites, does V appear to decrease in concentration with increasing differentiation as marked by increasing Yb concentrations. These same lavas also are characterized by decreasing TiO_2 concentrations with increasing differentiation. Thus, both Ti and V are compatible elements in these andesitic lavas, which can be attributed to magnetite fractionation.

[28] Progressive melting of the mantle will produce positively sloping curvilinear trends when one moderately incompatible element is plotted against another [e.g., *Gill*, 1981]. A straight line segment drawn through any portion of these trends will intersect the axis of the element with the higher partition coefficient. Based on plots of V against TiO_2 and Yb for basalts from ocean ridges, IBM back arcs, and the FAB (Figure 5), the bulk partition coefficient for V must be generally greater than those of Ti and heavy REE as represented by Yb during differentiation of basalts in extensional tectonic settings.

[29] The overall low TiO_2 and Yb concentrations compared to V for the FAB suggest that the more highly incompatible Ti and Yb are more depleted than the less incompatible V in the mantle sources for FAB compared to the sources of lavas from other extensional settings. The likely cause of this depletion was a melting event for the FAB source that did not affect the sources of IBM back-arc lavas. The cause and timing of this earlier melting event is uncertain. It is possible it was related to melting during early spreading in the WPB. If so, then the mantle that welled up to generate the WPB crust before about 51 Ma could have resided beneath the Mariana fore arc when the Pacific Plate began to subduct. However, this explanation is not obviously consistent with the radiogenic Nd isotopic compositions of some FAB compared to basalts from the WPB, nor with the differences in Nd and Hf isotopic compositions between the FAB and the boninites.

[30] An alternative mantle source for IBM fore-arc lavas could have been the lithosphere beneath Asia. Unusually low Os isotopic compositions in some highly depleted fore-arc peridotites have been attributed to eon-scale depletion in Re compared to Os [*Parkinson et al.*, 1998]. One potential origin for this mantle is subcontinental mantle from Asia that detached, became part of the asthenosphere, and convected into the area by southward or eastward directed mantle flow [*Parkinson et al.*, 1998; *Flower et al.*, 2001]. This introduced mantle could both be the source of the Indian Ocean MORB domain Nd-Hf-Pb isotope signatures found in IBM arc, back-arc, and fore-arc volcanics, and the convective flow could have pushed the young Philippine Plate over the old Pacific Plate, triggering failure of the Pacific Plate and subduction initiation [*Hall et al.*, 2003].

[31] The Nd isotopic compositions for FAB range from more radiogenic and transitional to a Pacific MORB-like mantle in the northwesterly dive sites to less radiogenic and Indian MORB-like in other locations. Thus, the mantle that decompressed to generate the FAB must have had ~100 km scale domains of mantle heterogeneity. This could have resulted from transfer of Nd from the newly subducting Pacific Plate in the northwesterly dive sites but not elsewhere, or variations in the Nd isotope values of the upwelling mantle. We favor the latter explanation because the most subduction affected FAB are those at the base of DSDP site 458, and these lavas have the Indian MORB domain Nd-Hf isotope signature.

[32] Our preferred hypothesis for the origin of IBM FAB is that they were the first lavas to erupt when the Pacific Plate began to sink beneath the Philippine Plate. They were generated from mantle rising to fill space created by the initial sinking of the Pacific Plate as first hypothesized by *Stern and Bloomer* [1992] and geodynamically modeled by *Hall et al.* [2003]. The source of the FAB was asthenospheric mantle that had characteristics ranging between those of the sources for Indian and Pacific Ocean MORB and melting was largely by decompression. The mild enrichments of fluid-soluble elements and radiogenic Pb and Sr isotope values for some FAB indicate that the decompression melting was sometimes enhanced by a flux of solute-bearing water driven off of the sinking Pacific Plate. Although the FAB source was more depleted than a normal MORB source in terms of REE and HFSE concentrations, the high CaO and Al_2O_3 concentrations and light-depleted REE patterns of the FAB suggest derivation from cpx-rich mantle. We therefore speculate that the upwelling of mantle associated with subduction initiation caused cpx-rich domains with high Sm/Nd and Lu/Hf to melt first, which resulted in generation of the FAB. The first FAB to erupt were those at the dive sites with basaltic SiO_2 concentrations and weak evidence for the involvement

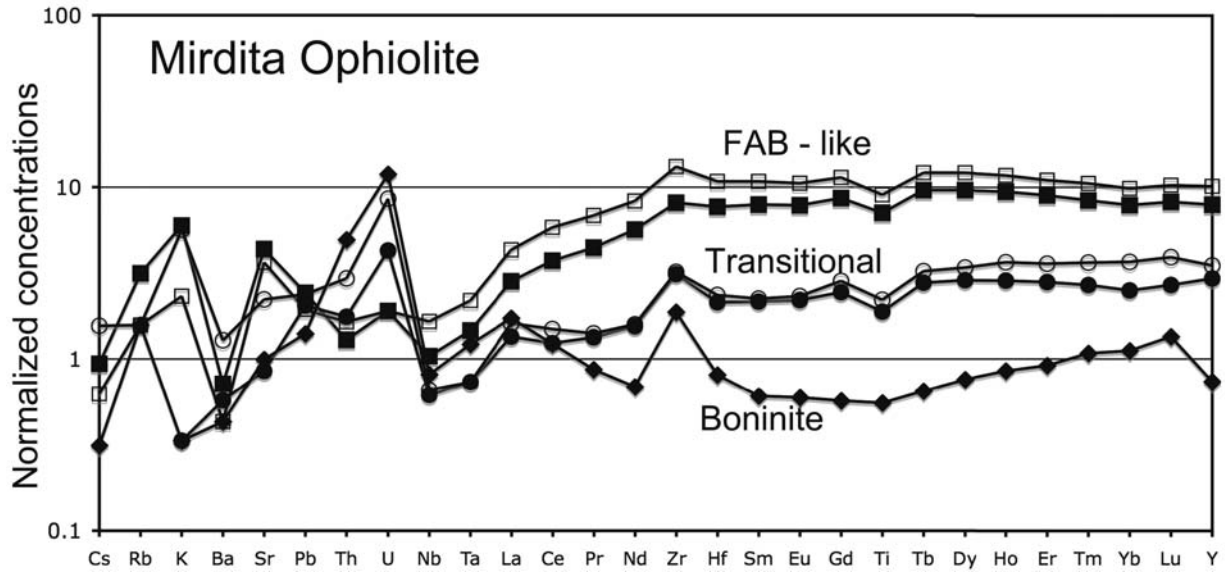

Figure 8. Primitive mantle normalized concentrations of incompatible trace elements for igneous rocks from the Mirdita ophiolite, Albania. Data are from *Dilek and Furnes* [2009]. Note the similarity of the trace element compositions between the Mirdita and DSDP site 458 and 459 illustrated in Figure 3b.

of the subducting slab. The FAB and transitional lavas from DSDP sites 458 and 459 are more silicic and have clear evidence that a subducted fluid was involved in their genesis. This suggests that later melting migrated to shallower levels and occurred after a water-rich subducted fluid was involved in their genesis.

[33] Boninite major element compositions require generation in the shallow mantle and in the presence of a water-rich fluid [*Falloon and Danyushevsky*, 2000; *Green*, 1973; *Parman and Grove*, 2004]. These compositions, as well as their low and often U-shaped REE concentrations and low Lu/Hf indicate that these boninites were generated from mantle that was harzburgitic and stripped of most incompatible elements. U, alkali metals, and other fluid-soluble elements are reenriched in the boninites source during melting [e.g., *Hickey and Frey*, 1982; *Hickey-Vargas*, 1989; *Ishizuka et al.*, 2006; *Stern and Bloomer*, 1992]. The relatively radiogenic Pb and Sr isotopic compositions of the boninites reflect this subducted component. The boninites, therefore, were generated from harzburgitic mantle domains with low Sm/Nd and Lu/Hf that were left after generation of the FAB and when a strong flux of fluid from the newly subducting Pacific slab became involved in magma genesis. The relatively unradiogenic Nd and Hf isotopic compositions of boninites compared to FAB suggest that differences in their Sm/Nd and Lu/Hf ratios were present in their sources long before subduction began, and that the cpx-rich and cpx-poor domains were too large to equilibrate isotopically during the FAB melting.

[34] The stratigraphic sequence in the SE Mariana fore arc is similar to those found in many ophiolites [*Shervais*, 2001; *Shervais et al.*, 2004]. For example, the Troodos [*Rogers et al.*, 1989; *Portnyagin et al.*, 1997], Oman [*Ishikawa et al.*, 2002], Mirdita [*Dilek et al.*, 2007; *Dilek et al.*, 2008], Pindos [*Dilek and Furnes*, 2009], Othris [*Barth and Gluhak*, 2009], and Kudi ophiolites [*Yuan et al.*, 2005] all have volcanic sections that include boninitic pillow lavas stratigraphically above tholeiitic basalts. The stratigraphic sections of the Mirdita and Pindos ophiolites are particularly similar to the IBM fore-arc stratigraphy in that the sheeted dikes are overlain progressively by MORB-like lavas, "island arc tholeiites" and related rocks, and boninites [*Dilek and Furnes*, 2009]. These island arc tholeiites have trace element patterns and isotopic compositions that are transitional between the MORB-like and boninite lavas, and therefore are stratigraphically and compositionally similar to those of the transitional lavas from DSDP site 458 (Figure 8). The similarity of the igneous rocks in the IBM fore arc and those in ophiolites supports the concept that the IBM fore arc is an in situ suprasubduction zone ophiolite [*Bloomer and Hawkins*, 1983; *Ishiwatari et al.*, 2006; *Stern*, 2004]. More importantly, this similarity suggests that broad-scale subduction initi-

ation could have been the progenitor of some regionally extensive ophiolitic provinces. Two potential examples are the Late Cretaceous and Middle to Late Jurassic Tethyan ophiolitic provinces [e.g., *Bortolotti and Principi*, 2005; *Dilek and Furnes*, 2009].

[35] The ~51 Ma age of FAB from the IBM is similar to the ~50 Ma age of the Hawaii-Emperor seamount bend. This age similarity has been used to link the change in Pacific Plate motion to subduction initiation in the western Pacific [e.g., *Sharp and Clague*, 2006]. This interval also was a period of major change in motion of the Australian plate, illustrating that forces can be transmitted to adjacent plates and significantly affect their motions [*Whittaker et al.*, 2007]. If subduction initiation events generated the Jurassic and Cretaceous Tethyan ophiolites, then they should have both contributed to closing the Tethyan Ocean and affected the motions of nearby plates. Evidence for significant changes in plate motion that coincide with ophiolite construction would therefore be supporting evidence for their genesis by subduction initiation. Both Tethyan ophiolite provinces do appear to have synchronous changes in plate motion. For example, the 95 Ma age of trondhjemites from the Oman ophiolite [*Warren et al.*, 2005] and a major plate reorganization that affected the former Gondwana region are synchronous [*Somoza and Zaffarana*, 2008]. Another apparent coincidence of ages are those of the Middle to Late Jurassic Tethyan ophiolites [e.g., *Bortolotti and Principi*, 2005] and rifting and eventual seafloor spreading along east Africa to open the Somali and Mozambique basins [*Storey*, 1995].

8. Conclusions

[36] The most abundant rock type between 2,000 and 6,500 m depth in the SE Mariana fore arc is tholeiitic basalt, which we term "fore-arc basalt" or FAB. These lavas have geochemical affinities with MORB and IBM back-arc lavas, but have lower Ti/V and Yb/V ratios reflecting a greater depletion in moderately incompatible elements in the FAB source mantle. The presence of lavas with transitional compositions between FAB and boninites, and the relatively radiogenic Pb and Sr isotopic compositions for some FAB suggest that these lavas are subduction related. Thus, we postulate that the FAB were the first lavas to erupt after the Pacific Plate began to subduct. The Hf and Nd isotopic compositions of most FAB link these magmas to a mantle source from the west whose easterly convection could have triggered this subduction initiation. The first mantle to melt from decompression generated FAB and had isotopic characteristics ranging from those similar to Pacific MORB source to Indian MORB source mantle. Later lavas appear to only have the Indian MORB domain signature. This partly reflects the harzburgitic nature of the source of the boninites, but probably also was the consequence of mantle flow through the newly formed mantle wedge, which eventually flushed out any remaining Pacific domain mantle.

[37] Geochemical similarities between the FAB to boninite sequence in the IBM fore arc and the shallow crustal sections of many ophiolites support the hypothesis that these ophiolites represent obducted fore-arc lithosphere generated during subduction initiation rather than back-arc or oceanic lithosphere. The similarity between the Mariana fore-arc stratigraphy and that found in Cretaceous and Jurassic Tethyan ophiolites suggest that these ophiolites also might have been associated with initiation of subduction that closed the Tethys ocean and affected plate motions of adjacent plates.

Acknowledgments

[38] We thank JAMSTEC for funding the cruises of the R/V *Yokosuka* and the *Shinkai 6500* diving. We also thank the *Shinkai 6500* and R/V *Yokosuka* crews for their outstanding work. U.S. scientific participation in *Shinkai* diving during 2006 and 2008 was supported by NSF grant 0827817 and a supplement to 0405651. NSF MARGINS grants OCE0001902 and EAR0840862 funded most of the other aspects of the U.S. participation in this research. J.B.T. acknowledges financial support from the French Institut National des Sciences de l'Univers. The isotope work at SDSU was supported by NSF grant OCE0001824. We thank Joan Miller and Catherine Baldridge for analytical support at SDSU. Arend Meijer provided DSDP samples. Terry Plank and David Mohler are thanked for help with LA-ICPMS analyses of glasses from the DSDP sites. Ben Ferreira is thanked for SEM photographs. Craig Lundstrom provided invaluable aid with the Hf isotope analyses at the University of Illinois. Constructive reviews by Yildirim Dilek and Jeff Ryan are greatly appreciated.

References

Barth, M. G., and T. M. Gluhak (2009), Geochemistry and tectonic setting of mafic rocks from the Othris Ophiolite, Greece, *Contrib. Mineral. Petrol.*, *157*, 23–40, doi:10.1007/s00410-008-0318-9.

Ben Othman, D., W. M. White, and J. Patchett (1989), The geochemistry of marine sediments, island arc magma genesis, and crust-mantle recycling, *Earth Planet. Sci. Lett.*, *94*, 1–21, doi:10.1016/0012-821X(89)90079-4.

Bortolotti, V., and G. Principi (2005), Tethyan ophiolites and Pangea break-up, *Isl. Arc*, *14*, 442–470, doi:10.1111/j.1440-1738.2005.00478.x.

Blichert-Toft, J., C. Chauvel, and F. Albarède (1997), Separation of Hf and Lu for high-precision isotope analysis of rock samples by magnetic sector multiple collector ICM-MS, *Contrib. Mineral. Petrol.*, *127*, 248–260, doi:10.1007/s004100050278.

Blichert-Toft, J., F. A. Frey, and F. Albarède (1999), Hf isotope evidence for pelagic sediments in the source of Hawaiian basalts, *Science*, *285*, 879–882, doi:10.1126/science.285.5429.879.

Bloomer, S. H. (1983), Distribution and origin of igneous rocks from the landward slopes of the Mariana Trench: Implications for its structure and evolution, *J. Geophys. Res.*, *88*(B9), 7411–7428, doi:10.1029/JB088iB09p07411.

Bloomer, S. H., and J. W. Hawkins (1983), Gabbroic and ultramafic rocks from the Mariana Trench; an island arc ophiolite, in *The Tectonic and Geologic Evolution of Southeast Asian Seas and Islands: Part 2*, *Geophys. Monogr. Ser.*, vol. 27, edited by D. E. Hayes, pp. 294–317, AGU, Washington, D. C.

Bloomer, S. H., and J. W. Hawkins (1987), Petrology and geochemistry of boninite series volcanic rocks from the Mariana Trench, *Contrib. Mineral. Petrol.*, *97*(3), 361–377, doi:10.1007/BF00371999.

Chauvel, C., and J. Blichert-Toft (2001), A hafnium isotope and trace element perspective on melting of the depleted mantle, *Earth Planet. Sci. Lett.*, *190*, 137–151, doi:10.1016/S0012-821X(01)00379-X.

Cosca, M., R. J. Arculus, J. A. Pearce, and J. G. Mitchell (1998), $^{40}Ar/^{39}Ar$ and K-Ar geochronological age constraints for the inception and early evolution of the Izu-Bonin-Mariana arc system, *Isl. Arc*, *7*, 579–595, doi:10.1111/j.1440-1738.1998.00211.x.

DeBari, S. M., B. Taylor, K. Spencer, and K. Fujioka (1999), A trapped Philippine Sea plate origin for MORB from the inner slope of the Izu-Bonin trench, *Earth Planet. Sci. Lett.*, *174*(1–2), 183–197, doi:10.1016/S0012-821X(99)00252-6.

Dilek, Y., and H. Furnes (2009), Structure and geochemistry of Tethyan ophiolites and their petrogenesis in subduction rollback systems, *Lithos*, *113*, 1–20, doi:10.1016/j.lithos.2009.04.022.

Dilek, Y., H. Furnes, and M. Shallo (2007), Suprasubduction zone ophiolite formation along the periphery of Mesozoic Gondwana, *Gondwana Res.*, *11*, 453–475, doi:10.1016/j.gr.2007.01.005.

Dilek, Y., H. Fumes, and M. Shallo (2008), Geochemistry of the Jurassic Mirdita Ophiolite (Albania) and the MORB to SSZ evolution of a marginal basin oceanic crust, *Lithos*, *100*, 174–209, doi:10.1016/j.lithos.2007.06.026.

Elliott, T., T. Plank, A. Zindler, W. White, and B. Bourdon (1997), Element transport from slab to volcanic front at the Mariana Arc, *J. Geophys. Res.*, *102*, 14,991–15,019.

Falloon, T. J., and L. V. Danyushevsky (2000), Melting of refractory mantle at 1.5, 2 and 2.5 GPa under anhydrous and H_2O-undersaturated conditions: Implications for the petrogenesis of high-Ca boninites and the influence of subduction components on mantle melting, *J. Petrol.*, *41*, 257–283, doi:10.1093/petrology/41.2.257.

Flower, M. F. J., R. M. Russo, K. Tamaki, and N. Hoang (2001), Mantle contamination and the Izu-Bonin-Mariana (IBM) 'high-tide mark': Evidence for mantle extrusion caused by Tethyan closure, *Tectonophysics*, *333*, 9–34, doi:10.1016/S0040-1951(00)00264-X.

Fryer, P., N. Becker, B. Appelgate, F. Martinez, M. Edwards, and G. Fryer (2003), Why is the Challenger Deep so deep?, *Earth Planet. Sci. Lett.*, *211*, 259–269, doi:10.1016/S0012-821X(03)00202-4.

Gill, J. B. (1981), *Orogenic Andesites and Plate Tectonics*, 390 pp., Springer, Berlin.

Graham, D. W., J. Blichert-Toft, C. J. Russo, K. H. Rubin, and F. Albarède (2006), Cryptic striations in the upper mantle revealed by hafnium isotopes in southeast Indian ridge basalts, *Nature*, *440*, 199–202, doi:10.1038/nature04582.

Green, D. H. (1973), Experimental melting studies on a model upper mantle composition at high pressure under water-saturated and water-undersaturated conditions, *Earth Planet. Sci. Lett.*, *19*, 37–53, doi:10.1016/0012-821X(73)90176-3.

Gvirtzman, Z., and R. J. Stern (2004), Bathymetry of Mariana trench-arc system and formation of the Challenger Deep as a consequence of weak plate coupling, *Tectonics*, *23*, TC2011, doi:10.1029/2003TC001581.

Hall, C. E., M. Gurnis, M. Sdrolias, L. L. Lavier, and R. D. Muller (2003), Catastrophic initiation of subduction following forced convergence across fracture zones, *Earth Planet. Sci. Lett.*, *212*, 15–30, doi:10.1016/S0012-821X(03)00242-5.

Hanan, B. B., and J.-G. Schilling (1989), Easter microplate evolution: Pb isotope evidence, *J. Geophys. Res.*, *94*, 7432–7448, doi:10.1029/JB094iB06p07432.

Hanan, B. B., J. Blichert-Toft, D. Pyle, and D. Christie (2004), Contrasting origins of the upper mantle MORB source revealed by Hf and Pb isotopes from the Australian-Antarctic Discordance, *Nature*, *432*, 91–94, doi:10.1038/nature03026.

Hickey, R. L., and F. A. Frey (1982), Geochemical characteristics of boninite series volcanics: Implications for their source, *Geochim. Cosmochim. Acta*, *46*, 2099–2115, doi:10.1016/0016-7037(82)90188-0.

Hickey-Vargas, R. (1989), Boninites and tholeiites from DSDP Site 458, Mariana Fore-arc, in *Boninites and Related Rocks*, edited by A. J. Crawford, pp. 339–356, Unwin Hyman, London.

Hickey-Vargas, R. (1991), Isotope characteristics of submarine lavas from the Philippine Sea: implications for the origin of arc and basin magmas of the Philippine tectonic plate, *Earth Planet. Sci. Lett.*, *107*, 290–304.

Hickey-Vargas, R. (1998), Origin of the Indian Ocean–type isotopic signature in basalts from Philippine Sea plate spreading centers: An assessment of local versus large-scale processes, *J. Geophys. Res.*, *103*, 20,963–20,979.

Hickey-Vargas, R., and M. K. Reagan (1987), Temporal variation of isotope and rare earth element abundances in volcanic rocks from Guam: Implications for the evolution of the Mariana Arc, *Contrib. Mineral. Petrol.*, *97*(4), 497–508, doi:10.1007/BF00375327.

Hussong, D. M., et al. (1982), *Initial Reports of the Deep Sea Drilling Project*, vol. 60, 929 pp., U.S. Govt. Print. Off., Washington, D. C.

Ishikawa, T., K. Ngaaishi, and S. Umino (2002), Boninitic volcanism in the Oman ophiolite: Implications for thermal condition during transition from spreading ridge to arc, *Geology*, *30*, 899–902, doi:10.1130/0091-7613(2002)030<0899:BVITOO>2.0.CO;2.

Ishiwatari, A., Y. Yanagida, Y.-B. Li, T. Ishii, S. Haraguchi, K. Koizumi, Y. Ichiyama, and M. Umeka (2006), Dredge petrology of the boninite- and adakite-bearing Hahajima Seamount of the Ogasawara (Bonin) fore-arc: An ophiolite or a serpentinite seamount?, *Isl. Arc*, *15*, 102–118, doi:10.1111/j.1440-1738.2006.00512.x.

Ishizuka, O., et al. (2006), Early stages in the evolution of Izu-Bonin Arc volcanism: New age, chemical, and isotopic constraints, *Earth Planet. Sci. Lett.*, *250*, 385–401, doi:10.1016/j.epsl.2006.08.007.

Ishizuka, O., M. Yuasa, I. Sakamoto, K. Kanayama, R. N. Taylor, S. Umino, K. Tani, and Y. Ohara (2008), Earliest Izu-Bonin arc volcanism found on the submarine Bonin Ridge, *Eos Trans. AGU*, *89*(53), Fall Meet. Suppl., Abstract V31A-2106.

Ishizuka, O., M. Yuasa, R. N. Taylor, and I. Sakamoto (2009), Two contrasting magmatic types coexist after the cessation of back-arc spreading, *Chem. Geol.*, *266*, 274–296, doi:10.1016/j.chemgeo.2009.06.014.

Johnson, D. M., P. R. Hooper, and R. M. Conrey (1999), Analysis of rocks and minerals for major and trace-elements on a single low dilution Li-tetraborate fused bead, *Adv. X Ray Anal.*, *41*, 843–867.

Karner, J. M., S. R. Sutton, J. J. Papike, C. K. Shearer, J. H. Jones, and M. Newville (2006), Application of a new vanadium valence oxybarometer to basaltic glasses from the Earth, Moon, and Mars, *Am. Mineral.*, *91*, 270–277, doi:10.2138/am.2006.1830.

Kelley, K. A., T. Plank, J. Ludden, and H. Staudigal (2003), Composition of altered oceanic crust at ODP Sites 801 and 1149, *Geochem. Geophys. Geosyst.*, *4*(6), 8910, doi:10.1029/2002GC000435.

Kempton, P. D., J. A. Pearce, T. L. Barry, J. G. Fitton, C. Langmuir, and D. M. Christie (2002), Sr-Nd-Pb-Hf Isotope Results from ODP Leg 187: Evidence for Mantle Dynamics of the Australian-Antarctic Discordance and Origin of the Indian MORB Source, *Geochem. Geophys. Geosyst.*, *3*(12), 1074, doi:10.1029/2002GC000320.

Komatsu, M. (1980), Clinoenstatite in volcanic rocks from the Bonin Islands, *Contrib. Mineral. Petrol.*, *74*, 329–338.

Kuroda, N., and K. Shiraki (1975), Boninite and related rocks of Chichijima, Bonin Islands, Japan, *Rep. Faculty Sci. Shizuoka Univ.*, *10*, 145–155.

Lee, C.-T. A., W. P. Leeman, D. Canil, and Z.-X. A. Li (2005), Similar V/Sc systematics in MORB and arc basalts: Implications for the oxygen fugacities of their mantle source regions, *J. Petrol.*, *46*, 2313–2336, doi:10.1093/petrology/egi056.

Lu, Y., A. Makishima, and E. Nakamura (2007), Purification of Hf in silicate materials using extraction chromatographic resin, and its application to precise determination of $^{176}Hf/^{177}Hf$ by MC-ICP-MS with ^{179}Hf spike, *J. Anal. At. Spectrom.*, *22*, 69–76, doi:10.1039/b610197f.

Martinez, F., P. Fryer, and N. Becker (2000), Geophysical characteristics of the southern Mariana Trough, *J. Geophys. Res.*, *105*, 16,591–16,607.

Meijer, A. (1976), Pb and Sr isotopic data bearing on the origin of volcanic rocks from the Mariana island-arc system, *Geol. Soc. Am. Bull.*, *87*, 1358–1369, doi:10.1130/0016-7606(1976)87<1358:PASIDB>2.0.CO;2.

Meijer, A. (1980), Primitive arc volcanism and a boninite series; example from western Pacific Island arcs, in *The Tectonic and Geologic Evolution of Southeast Asian Seas and Islands*, *Geophys. Monogr. Ser.*, vol. 23, edited by D. E. Hayes, pp. 269–282, AGU, Washington, D. C.

Meijer, A., E. Anthony, and M. Reagan (1982), Petrology of the fore-arc sites, *Initial Rep. Deep Sea Drill. Proj.*, *60*, 709–730.

Meijer, A., M. Reagan, H. Ellis, M. Shafiqullah, J. Sutter, P. Damon, and S. Kling (1983), Chronology of volcanic events in the eastern Philippine Sea, in *The Tectonic and Geologic Evolution of Southeast Asian Seas and Islands: Part 2*, *Geophys. Monogr. Ser.*, vol. 27, edited by D. E. Hayes, pp. 349–359, AGU, Washington, D. C.

Münker, C., S. Weyer, E. Scherer, and K. Mezger (2001), Separation of high field strength elements (Nb, Ta, Zr, Hf) and Lu from rock samples for MC-ICPMS measurements, *Geochem. Geophys. Geosyst.*, *2*(12), 1064, doi:10.1029/2001GC000183.

Ohara, Y., et al. (2008), Studies of the Southern Izu-Bonin-Mariana (IBM) fore-arc using Shinkai 6500: Watery glimpses of an in situ fore-arc ophiolite, *Eos Trans. AGU*, *89*(53), Fall Meet. Suppl., Abstract V33A-2194.

Parkinson, I. J., C. J. Hawkesworth, and A. S. Cohen (1998), Ancient mantle in a modern arc: Osmium isotopes in Izu-Bonin-Mariana fore-arc peridotites, *Science*, *281*, 2011–2014, doi:10.1126/science.281.5385.2011.

Parman, S. W., and T. L. Grove (2004), Harzburgite melting with and without H_2O: Experimental data and predictive modeling, *J. Geophys. Res.*, *109*, B02201, doi:10.1029/2003JB002566.

Pearce, J. A., M. F. Thirlwall, G. Ingram, B. J. Murton, R. J. Arculus, and S. R. van der Laan (1992), Isotopic evidence for the origin of boninites and related rocks drilled in the Izu-Bonin (Ogasawara) fore-arc, Leg 125, *Proc. Ocean Drill. Program Sci. Results*, *125*, 237–261.

Pearce, J. A., P. D. Kempton, G. M. Nowell, and S. R. Noble (1999), Hf-Nd element and isotope perspective on the nature and provenance of mantle and subduction components in Western Pacific arc-basin systems, *J. Petrol.*, *40*, 1579–1611, doi:10.1093/petrology/40.11.1579.

Plank, T., and J. N. Ludden (1992), Geochemistry of sediments in the Argo abyssal plain at Site 765; a continental margin reference section for sediment recycling in subduction zones, *Proc. Ocean Drill. Program Sci. Results*, *123*, 167–189.

Portnyagin, M. V., L. V. Danyushevsky, and V. S. Kamenetsky (1997), Coexistence of two distinct mantle sources during formation of ophiolites: A case study of primitive pillow-lavas from the lowest part of the volcanic section of the Troodos Ophiolite, Cyprus, *Contrib. Mineral. Petrol.*, *128*, 287–301, doi:10.1007/s004100050309.

Reagan, M. K., and A. Meijer (1984), Geology and geochemistry of early arc-volcanic rocks from Guam, *Geol. Soc. Am. Bull.*, *95*(6), 701–713, doi:10.1130/0016-7606(1984)95<701:GAGOEA>2.0.CO;2.

Reagan, M. K., B. B. Hanan, M. T. Heizler, B. S. Hartman, and R. Hickey-Vargas (2008), Petrogenesis of volcanic rocks from Saipan and Rota, Mariana Islands, and implications for the evolution of nascent island arcs, *J. Petrol.*, *49*, 441–464, doi:10.1093/petrology/egm087.

Rogers, N. W., C. J. MacLeod, and B. J. Murton (1989), Petrogenesis of boninitic lavas from the Limassol Forrest Complex, in *Boninites and Related Rocks*, edited by A. J. Crawford, pp. 289–313, Unwin-Hyman, London.

Rowe, M. C., A. J. R. Kent, and R. L. Nielsen (2007), Determination of sulfur speciation and oxidation state of olivine hosted melt inclusions, *Chem. Geol.*, *236*, 303–322, doi:10.1016/j.chemgeo.2006.10.007.

Savov, I. P., R. Hickey-Vargas, M. D'Antonio, J. G. Ryan, and P. Spaeda (2006), Petrology and geochemistry of West Philippine Basin Basalts and Early Palau–Kyushu Arc volcanic clasts from ODP Leg 195, Site 1201D: Implications for the early history of the Izu–Bonin–Mariana Arc, *J. Petrol.*, *47*, 277–299, doi:10.1093/petrology/egi075.

Sharp, W. D., and D. A. Clague (2006), 50-Ma initiation of Hawaiian-Emperor bend records major change in Pacific Plate motion, *Science*, *313*, 1281–1284, doi:10.1126/science.1128489.

Shervais, J. W. (1982), Ti-V plots and the petrogenesis of modern and ophiolitic lavas, *Earth Planet. Sci. Lett.*, *59*, 101–118, doi:10.1016/0012-821X(82)90120-0.

Shervais, J. W. (2001), Birth, death, and resurrection: The life cycle of suprasubduction zone ophiolites, *Geochem. Geophys. Geosyst.*, *2*(1), 1010, doi:10.1029/2000GC000080.

Shervais, J. W., D. L. Kimbrough, P. Renne, B. B. Hanan, B. Murchey, C. A. Snow, M. M. Zoglman Schuman, and J. Beaman (2004), Multi-stage origin of the Coast Range Ophiolite, California: Implications for the life cycle of supra-subduction zone ophiolites, *Int. Geol. Rev.*, *46*, 289–315, doi:10.2747/0020-6814.46.4.289.

Somoza, R., and C. B. Zaffarana (2008), Mid-Cretaceous polar standstill of South America, motion of the Atlantic hotspots and the birth of the Andean Cordillera, *Earth Planet. Sci. Lett.*, *271*, 267–277, doi:10.1016/j.epsl.2008.04.004.

Staudigel, H., K.-H. Park, M. Pringle, J. L. Rubenstone, W. H. F. Smith, and A. Zindler (1991), The longevity of the South Pacific isotopic and thermal anomaly, *Earth Planet. Sci. Lett.*, *102*, 24–44, doi:10.1016/0012-821X(91)90015-A.

Stern, R. J. (2004), Subduction initiation; spontaneous and induced, *Earth Planet. Sci. Lett.*, *226*, 275–292.

Stern, R. J., and S. H. Bloomer (1992), Subduction zone infancy; examples from the Eocene Izu-Bonin-Mariana and Jurassic California arcs, *Geol. Soc. Am. Bull.*, *104*, 1621–1636, doi:10.1130/0016-7606(1992)104<1621:SZIEFT>2.3.CO;2.

Storey, B. C. (1995), The role of mantle plumes in continental breakup: Case histories from Gondwanaland, *Nature*, *377*, 301–308, doi:10.1038/377301a0.

Sun, S. S., and W. F. McDonough (1989), Chemical and isotopic systematics of oceanic basalts; implications for mantle composition and processes, in *Magmatism in the Ocean Basins*, edited by A. D. Saunders, *Geol. Soc. Spec. Publ.*, *42*, 313–345.

Taylor, R. N., and R. W. Nesbitt (1994), Arc volcanism in an extensional regime at the initiation of subduction: A geochemical study of Hahajima, Bonin Islands, Japan, *Geol. Soc. Spec. Publ.*, *81*, 115–134, doi:10.1144/GSL.SP.1994.081.01.07.

Taylor, R. N., R. W. Nesbitt, P. Vidal, R. S. Harmon, B. Auvray, and I. W. Croudace (1994), Mineralogy, chemistry, and genesis of the boninite series volcanics, Chichijima, Bonin Islands, Japan, *J. Petrol.*, *35*, 577–617.

Ulfbeck, D., J. Baker, T. Waight, and E. Krogstad (2003), Rapid sample digestion by fusion and chemical separation of Hf for isotopic analysis by MC-ICPMS, *Talanta*, *59*, 365–373, doi:10.1016/S0039-9140(02)00525-8.

Umino, S. (1985), Volcanic geology of Chichijima, the Bonin Islands (Ogasawara Islands), *J. Geol. Soc. Jpn.*, *91*, 505–523.

Volpe, A. M., J. D. Macdougall, G. W. Lugmair, J. W. Hawkins, and P. F. Lonsdale (1990), Fine-scale isotopic variation in Mariana Trough basalts: Evidence for heterogeneity and a recycled component in backarc basin mantle, *Earth Planet. Sci. Lett.*, *100*, 251–264.

Warren, C. J., R. R. Parrish, D. J. Waters, and M. P. Searle (2005), Dating the geologic history of Oman's Semail ophiolite: Insights from U-Pb geochronology, *Contrib. Mineral. Petrol.*, *150*, 403–422, doi:10.1007/s00410-005-0028-5.

White, W. M., et al. (2000), High-precision analysis of Pb isotope ratios by multicollector ICP-MS, *Chem. Geol.*, *167*, 257–270, doi:10.1016/S0009-2541(99)00182-5.

Whittaker, J. M., R. D. Müller, G. Leitchenkov, H. Stagg, M. Sdrolias, C. Gaina, and A. Goncharov (2007), Major Australian-Antarctic plate reorganization at Hawaiian-Emperor bend time, *Science*, *318*, 83–86, doi:10.1126/science.1143769.

Woodhead, J. D., J. M. Hergt, J. P. Davidson, and S. M. Eggins (2001), Hafnium isotope evidence for "conservative" element mobility during subduction zone processes, *Earth Planet. Sci. Lett.*, *192*, 331–346, doi:10.1016/S0012-821X(01)00453-8.

Yuan, C., M. Sun, M.-F. Zhou, W. Xiao, and H. Zhou (2005), Geochemistry and petrogenesis of the Yishak Volcanic Sequence, Kudi ophiolite, West Kunlun (NW China): Implications for the magmatic evolution in a subduction zone environment, *Contrib. Mineral. Petrol.*, *15*, 195–211, doi:10.1007/s00410-005-0012-0.